Ultrasound Obstet Gynecol 2022; **59**: 358–364
Published online in Wiley Online Library (wileyonlinelibrary.com). **DOI:** 10.1002/uog.23753.

B-flow/spatiotemporal image correlation M-mode: novel ultrasound method that detects decrease in spiral artery luminal diameter in first trimester in primate model of impaired spiral artery remodeling

O. M. TURAN[1], J. S. BABISCHKIN[1], G. W. ABERDEEN[1], S. TURAN[1], C. R. HARMAN[1], G. J. PEPE[2] and E. D. ALBRECHT[1]

[1]*Department of Obstetrics, Gynecology and Reproductive Sciences, University of Maryland School of Medicine, Baltimore, MD, USA;*
[2]*Department of Physiological Sciences, Eastern Virginia Medical School, Norfolk, VA, USA*

KEYWORDS: B-flow; M-mode; primate; remodeling; spiral artery diameter; STIC; ultrasound; uterine

CONTRIBUTION

What are the novel findings of this work?
B-flow/spatiotemporal image correlation (STIC) M-mode ultrasonography provides a novel, safe, real-time technology to quantify in the first trimester of baboon pregnancy a decrease in spiral artery luminal diameter, reflecting decreased distensibility of the vessel wall, as an index of impaired spiral artery remodeling (SAR).

What are the clinical implications of this work?
B-flow/STIC M-mode ultrasonography has the potential to be used as a screening tool to ascertain and evaluate the efficacy of new therapeutic modalities to prevent a defect in SAR early in gestation in women who go on to exhibit pregnancy complications.

ABSTRACT

Objective *To determine if B-flow/spatiotemporal image correlation (STIC) M-mode ultrasonography detects a decrease in spiral artery luminal diameter and volume flow during the first trimester in a non-human primate model of impaired spiral artery remodeling (SAR).*

Methods *Pregnant baboons were treated daily with estradiol benzoate on days 25–59 of the first trimester (term, 184 days), or remained untreated. On day 60 of gestation, spiral artery luminal diameter (in seven untreated and 12 estradiol-treated baboons) and volume flow (in four untreated and eight estradiol-treated baboons) were quantified by B-flow/STIC M-mode ultrasonography. In addition, in 15 untreated and 18 estradiol-treated baboons, the percent of spiral arteries remodeled by extravillous trophoblasts was quantified* ex vivo *by immunohistochemical image analysis on placental basal plate tissue collected via Cesarean section on day 60. Findings were compared between treated and untreated animals. The correlation between spiral artery luminal diameter and percent of SAR was assessed in three untreated and six estradiol-treated baboons which underwent both B-flow/STIC M-mode ultrasound and quantification of SAR.*

Results *The proportion of spiral arteries greater than 50 μm in diameter remodeled by extravillous trophoblasts was 70% lower in estradiol-treated baboons than in untreated animals (*$P = 0.000001$*). Spiral artery luminal diameter in systole and diastole, as quantified by B-flow/STIC M-mode in the first trimester of pregnancy, was 31% (*$P = 0.014$*) and 50% (*$P = 0.005$*) lower, respectively, and volume flow was 85% lower (*$P = 0.014$*), in SAR-suppressed baboons compared with untreated animals. There was a significant correlation between spiral artery luminal diameter as quantified by B-flow/STIC M-mode ultrasonography and the percent of SAR (*$P < 0.05$*).*

Conclusion *B-flow/STIC M-mode ultrasonography provides a novel real-time non-invasive method to detect a decrease in uterine spiral artery luminal diameter and volume flow during the cardiac cycle, reflecting decreased distensibility of the vessel wall, in the first trimester in a non-human primate model of defective SAR.* © *2021 The Authors. Ultrasound in Obstetrics & Gynecology published by John Wiley & Sons Ltd on behalf of International Society of Ultrasound in Obstetrics and Gynecology.*

Correspondence to: Dr E. D. Albrecht, Department of Obstetrics, Gynecology and Reproductive Sciences, University of Maryland School of Medicine, Baltimore, MD 21201, USA (e-mail: ealbrecht@som.umaryland.edu)

Accepted: 26 July 2021

INTRODUCTION

During the first trimester of pregnancy, the uterine spiral arteries are remodeled by extravillous trophoblasts into high-capacity vessels with enlarged lumens to promote placental perfusion. A defect in spiral artery remodeling (SAR) underlies early-onset pre-eclampsia, fetal growth restriction and preterm birth[1–3]. Non-invasive real-time imaging methods to assess spiral artery dynamics that reflect impaired SAR early in gestation would be invaluable to diagnose abnormal human pregnancy caused by defective SAR. However, an *in-vivo* assessment tool that can reliably quantify impaired SAR has not been developed. Although uterine artery flow resistance is currently used as a proxy marker for impaired placentation, its value in the first and second trimesters as a standalone test is limited[4–6]. Histological studies show clearly that extensively remodeled spiral arteries have a thin wall that accommodates increased blood flow, whereas poorly remodeled vessels retain a thickened wall and narrow lumen[7]. However, histological detection of impaired SAR can be made only in tissue obtained after birth[1,2] and, thus, is not of timely use to predict at-risk pregnancy. Since the main change in SAR is in the blood-vessel architecture, an imaging method that could quantify vessel dimension in real time, reflecting the movements of the vessel wall against blood flow during the cardiac cycle, would be the best test to identify differences in proper and improper SAR. In addition, the method should be validated with immunohistochemical assessment of the level of SAR at the time of imaging.

We have established, by slightly elevating estradiol levels early in baboon pregnancy, a highly specific, selective and reproducible model of defective SAR[8,9]. Pregnant baboons exhibit similar uterine vascular anatomy, maternal–placental–fetal endocrine axis and SAR to those in human pregnancy[10]. In the baboon model, impaired SAR was associated late in gestation with reduced uterine artery flow, increased maternal serum soluble fms-like tyrosine kinase-1 (sFlt-1) levels, maternal hypertension and maternal vascular endothelial dysfunction, which are all hallmarks of human pre-eclampsia[8,9,11–13]. We propose that this primate paradigm provides an innovative model to establish new real-time imaging approaches to assess aspects of SAR.

B-flow ultrasound is a non-Doppler technology for assessing vessels of the fetal heart and other organs[14–16]. B-flow provides high-contrast resolution for sharp rendering of vessel structure; however, it does not allow for functional measurements. Spatiotemporal image correlation (STIC) reconstructs a volumetric dataset from over 1500 image slices in five transverse planes and synchronizes volumetric data with the pulse. M-mode ultrasound generates spatial information along the sound beam axis with high temporal resolution to quantify digitally vessel dimension/diameter. We hypothesize that the spiral artery wall luminal diameter, which reflects the distensibility of the vessel wall during systole and diastole, is lower in poorly remodeled spiral arteries. To test this hypothesis, we combined B-flow/STIC with M-mode to quantify spiral artery luminal diameter during systole and diastole and compared imaging results with *ex-vivo* immunohistochemical quantification of SAR during the first trimester of baboon pregnancy.

METHODS

Animals

The present study was conducted in accordance with the ARRIVE (Animal Research: Reporting of *In Vivo* Experiments) guidelines[17] to enable evaluation of the rigor and reproducibility of the methods, statistical analysis and results. Baboons *(Papio anubis)* were obtained from the Southwest National Primate Research Center (San Antonio, TX, USA), housed individually in large primate cages, and received standard primate chow (Teklad Primate Diet 2050; Envigo, Frederick, MD, USA) and fresh fruit twice daily and water *ad libitum*. Female baboons were paired with male baboons for 5 days at the anticipated time of ovulation as estimated by menstrual cycle history and the pattern of external sex skin turgescence. Day 1 of pregnancy was designated as the day preceding perineal deturgescence. Baboons were cared for and used strictly in accordance with the United States Department of Agriculture regulations and the National Institutes of Health Guide for the Care and Use of Laboratory Animals (8th ed.)[18]. The present experimental protocol was approved by the Institutional Animal Care and Use Committee of the University of Maryland School of Medicine (approval number: 0220005).

Pregnant baboons were treated daily on days 25–59 of gestation with estradiol benzoate (25 μg/kg of body weight/day subcutaneously in 1.0 mL of sesame oil) or remained untreated. The length of gestation is 184 days in baboons. On day 60 of gestation (i.e. near the end of the first trimester), the baboons were lightly anesthetized with propofol/ketamine administered intravenously and supplemented with oxygen (1 L/min) to maintain oxygen saturation > 95% and blood pressure and heart rate constant. B-flow/STIC M-mode ultrasound imaging of the uterine spiral arteries was performed as described below in seven untreated and 12 estradiol-treated baboons. Fifteen untreated and 18 estradiol-treated baboons were anesthetized with isoflurane and, subsequently, blood samples (2 mL) were obtained from the maternal saphenous vein and the placenta was removed by Cesarean section for immunohistochemical quantification of SAR. Both B-flow/STIC M-mode ultrasound and quantification of SAR were performed in nine of these baboons (three untreated and six estradiol-treated), because some baboons were carried to term as part of another study or ultrasound imaging could not be performed. Serum estradiol levels were determined by radioimmunoassay using an automated chemiluminescent immunoassay system (Immulite; Diagnostic Products Corp., Los Angeles, CA, USA) to confirm estradiol treatment. Intra-assay and interassay coefficients of variation were 6.9% and 7.3%, respectively.

Ultrasound B-flow/STIC M-mode quantification of spiral artery luminal diameter and volume flow

Ultrasound B-flow/STIC M-mode imaging was performed using a GoldSeal Voluson E8 ultrasound machine with a three-/four-dimensional (3D/4D) transducer (RAB6-D ultralight, 4–8.5 MHz STIC Convex) (GE Healthcare, Zipf, Austria). Figure 1 illustrates the B-flow/STIC M-mode technique. Spiral arteries in the decidua basalis were identified in an untreated baboon using power and pulse Doppler (Figure 1a). The spiral artery location was selected systemically at 2–4-cm interval sectors starting from the site of cord insertion in the placenta (defined as the origin). Following B-flow activation, the same spiral artery was located (Figure 1b). Volume datasets representing multiplanar sequences of the vessels were then acquired in 4D-STIC mode (10 s, 25° angle). Archived 4D block images were obtained from six randomly selected regions, using a computer-generated number sequence[19] to minimize bias, for offline quantification of vessel diameters. Post-processing analyses were performed utilizing 4D View (GE Healthcare) and the multiplanar modality, which allows for simultaneous display of images in three orthogonal planes (which correspond to the *x*-, *y*- and *z*-axes) (Figure 1c). Image magnification was adjusted to 1.8 and, upon identification of the same vessel in each dimensional plane, M-mode was activated with a sweep speed of 2 mm/s. M-mode gate was positioned on the vessel perpendicular (90°) to the vessel lumen, and the vessel luminal diameter, reflecting the wall movement during systole and diastole, was determined (Figure 1d). The arterial luminal diameter reaches a maximum in mid-systole, which is immediately after peak arterial pressure, and the vessel luminal diameter decreases towards end-diastole as pressure declines. The luminal diameters of the vessel at the largest (systole) and smallest (diastole) segments were measured using a caliper and expressed in mm. Using the M-mode time measurement function, the duration of systole and diastole were measured and expressed in ms. Each spiral artery was measured three times, and the mean of the three measurements was assigned as the diameter of the blood vessel lumen during elapsed time for systole and diastole. The mean (± standard error) coefficient of variation for repeat B-flow/STIC M-mode measurements of the luminal diameter of each vessel in systole was 7.9 ± 1.1%. The minimum detectable luminal diameter of a spiral

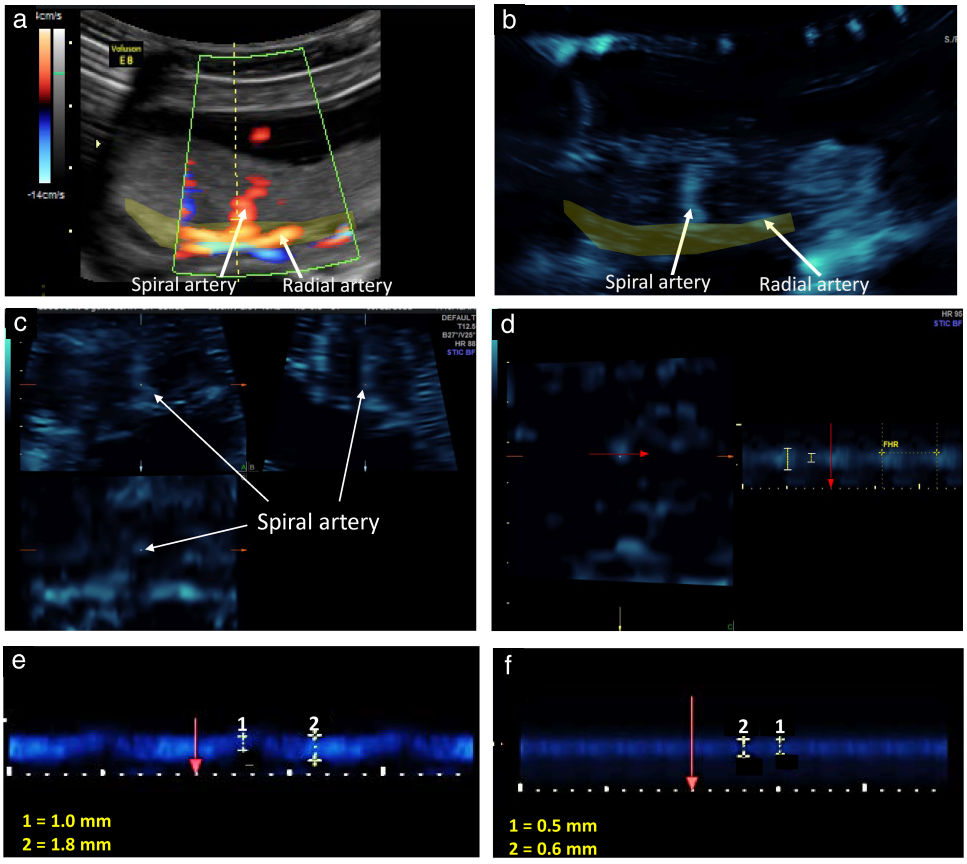

Figure 1 (a–d) Measurement of spiral artery luminal diameter using the B-flow/STIC M-mode technique in an untreated baboon on day 60 of gestation: (a) a spiral artery was identified in the placental bed (yellow shaded area) using power Doppler; (b) B-flow was activated and the spiral artery was demonstrated at the same anatomical location; (c) a 4D-STIC block was acquired and the spiral artery was visualized in the three orthogonal planes; (d) during post-processing, M-mode was activated at the *z*-axis and the spiral artery luminal diameter was measured perpendicular (red arrow) to the vessel lumen. Fetal heart rate was measured each time to confirm that the blood vessel was a maternal vessel. (e,f) Representative B-flow/STIC M-mode measurement of spiral artery luminal diameter during the cardiac cycle (1: diastole, 2: systole) in an untreated baboon (e) and in a baboon with spiral artery remodeling impairment following estradiol treatment (f).

artery, as assessed by B-flow/STIC M-mode in early baboon pregnancy, approximated 0.1 mm. Figure 1e,f shows B-flow/STIC M-mode measurement of spiral artery luminal diameter in (1) diastole and (2) systole in a remodeled distensible spiral artery of an untreated baboon (Figure 1e) and a non-remodeled spiral artery in a SAR-suppressed baboon (Figure 1f). The luminal diameter of the vessel in the SAR-impaired baboon was lower in systole (0.6 mm) and in diastole (0.5 mm) than that of the vessel in the untreated animal (1.8 mm and 1.0 mm, respectively).

Volume flow was calculated using the following formula: $\pi \times (D/2)^2 \times ((S \times T_S) + (D \times T_D))/(T_S + T_D)$, where S is systolic diameter, D is diastolic diameter, T_S is time for systole and T_D is time for diastole. All B-flow/STIC M-mode measurements were performed by a single investigator (O.M.T.).

The following criteria ensured B-flow/STIC M-mode authentication, optimization, standardization and quality control: (1) the spiral artery was visible in all three dimensions within the field of the acquired block; (2) the gate of the M-mode was positioned at 90° to the vessel lumen; (3) quantification of the luminal diameter in systole and diastole determined by pulse-Doppler measurement of heart rate was compared with the maternal pulse; (4) independence of the transmission angle and almost artifact-free depiction of artery structure to ensure accurate high-resolution assessment of vessel dimension; (5) correlation of visual pulsatility identified in the artery was depicted with the documented arterial pulse; and (6) arteries were differentiated from veins by their flow properties. Of note, spiral artery luminal diameter and volume flow, as determined by B-flow/STIC M-mode, were similar in the area of cord insertion and near the margins of the placenta.

In an ongoing companion study of B-flow/STIC M-mode in human subjects, obtaining the 4D block images added 5–8 min to the routine ultrasound examination in the first, second and third trimesters, while offline post-processing analysis took 20–30 min per subject. If the offline measurements are completed at the time of obtaining the 4D block, the total exam would be prolonged by only 15–20 min. B-flow/STIC M-mode imaging of the spiral arteries in the pregnant baboon takes a total of 30–45 min for the entire process due to challenges of the small size of the placenta in the first trimester.

Immunohistochemical quantification of uterine spiral artery remodeling

SAR was quantified by immunohistochemical imaging in 15 untreated and 18 estradiol-treated baboons. A minimum of six randomly selected areas (5 mm^3) of placental basal plate were collected from each baboon for SAR analysis. Placental samples were fixed in 10% formalin, embedded in paraffin, sectioned (5 μm), and processed for hematoxylin/eosin histology and cytotrophoblast/epithelial cell-specific cytokeratin immunohistochemistry (12.5 mg/mL, 345 779 CAM 5.2; BD Biosciences, San Jose, CA, USA). Light microscopy (Nikon Eclipse E 1000 M; Tokyo, Japan) and an image analysis system (IP Lab version 3.63; Scanalytics, Inc., Fairfax, VA, USA) were used to quantify the level of SAR in arteries of > 50 μm in diameter within the decidua basalis in each tissue sample, as described previously[8,9]. Vessel diameter was assessed via a micrometer as the smallest distance across the center of the vessel lumen from the inside edge of the surrounding smooth muscle (not invaded) or cytotrophoblast (invaded) layers. The number of arteries exhibiting trophoblast invasion and remodeling was quantified by identifying spiral arteries in which the vessel wall was extensively ($> 50\%$) occupied by cytokeratin-positive cytotrophoblasts. Data were expressed as the percent of SAR, i.e. the number of trophoblast remodeled arteries divided by the total number of arteries counted. Although there were spiral arteries in which $< 50\%$ of the vessel wall was occupied by trophoblasts, presumably reflecting partial adaptation, the numbers of these vessels were not quantified by immunohistochemical image analysis.

Statistical analysis

Data were analyzed using Student's *t*-test for independent observations using GraphPad software (San Diego, CA, USA). The baboon placenta consists of approximately 20 cotyledons[20,21], each supplied via a single spiral artery[22]. Each rendered B-flow/STIC M-mode image contained one to three different vessels, and 4–10 spiral arteries were measured per animal, or a total of 46 arteries in the untreated and 81 arteries in the estradiol-treated baboons were analyzed by B-flow/STIC M-mode imaging. The percent of SAR, as quantified by immunohistochemical image analysis, was obtained in a minimum of 12 spiral arteries per animal. Spiral artery luminal diameter, as quantified by B-flow/STIC M-mode, was correlated by linear regression with the percent of SAR, as quantified by immunohistochemical image analysis.

RESULTS

In the seven untreated and 12 estradiol-treated baboons that underwent B-flow/STIC M-mode imaging, mean maternal saphenous vein serum estradiol levels on day 60 of gestation were approximately 4-fold higher ($P < 0.01$) in estradiol-treated baboons compared with the untreated animals. Maternal mean arterial blood pressure, placental weight and fetal body weight were not significantly different between the two groups (Table 1).

In the 15 untreated and 18 estradiol-treated baboons in which SAR was quantified by immunohistochemical image analysis, the median (interquartile range (IQR)) value for the percent of SAR by extravillous trophoblasts was approximately 70% lower in the estradiol-treated baboons compared with the untreated animals (11.52 (5.38–18.02)% *vs* 33.00 (28.60–46.80)%; $P = 0.000001$) (Figure 2).

In the seven untreated and 12 estradiol-treated baboons that underwent B-flow/STIC M-mode ultrasonography, the median (IQR) value for spiral artery luminal diameter in systole was 31% lower in the SAR-impaired baboons compared with the untreated animals (1.1 (0.8–1.6) mm *vs* 1.6 (1.5–2.2) mm; $P = 0.014$) (Figure 3a). Moreover, the median (IQR) value for spiral artery luminal diameter in diastole was 50% lower in the SAR-suppressed compared with the untreated baboons (0.5 (0.4–0.8) mm *vs* 1.0 (0.8–1.1) mm; $P = 0.005$) (Figure 3b). B-flow/STIC M-mode imaging and *ex-vivo* quantification of the level of SAR were performed simultaneously in nine of the untreated and estradiol-treated baboons. As shown in Figure 4, there was a significant correlation between spiral artery luminal diameter as quantified in systole by B-flow/STIC M-mode and the percent of SAR quantified by immunohistochemical image analysis ($r = 0.67$; slope = 0.029; $P < 0.05$).

Table 1 Maternal saphenous vein serum estradiol levels, mean arterial blood pressure (MAP) and placental and fetal body weights on day 60 of gestation (term, 184 days) in seven untreated baboons and 12 baboons treated with estradiol benzoate, that underwent B-flow/STIC M-mode ultrasound imaging of the uterine spiral arteries

Parameter	*No treatment* (n = *7*)	*Estradiol* (n = *12*)
Estradiol (ng/mL)	0.22 ± 0.02	0.81 ± 0.06*
MAP (mmHg)	71 ± 6	72 ± 5
Placental weight (g)	31.6 ± 0.3	28.4 ± 0.5
Fetal body weight (g)	12.1 ± 0.2	11.5 ± 0.1

Data are given as mean ± standard error. *$P < 0.01$ compared with untreated baboons.

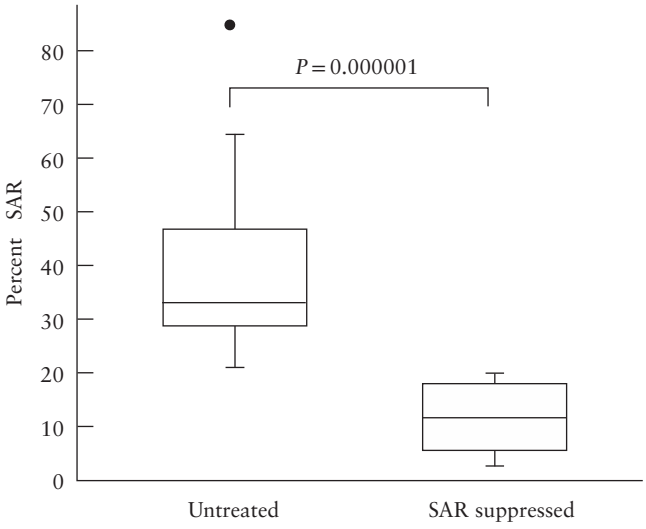

Figure 2 Box-and-whiskers plots showing percent of spiral artery remodeling (SAR) (i.e. the number of trophoblast-invaded arteries divided by the total number of arteries counted), as quantified by immunohistochemical image analysis, for vessels > 50 µm in diameter, on day 60 of gestation, in 15 untreated and 18 SAR-suppressed baboons. Boxes are median and interquartile range (IQR) and whiskers are range excluding one outlier (●) more than 1.5 × IQR from upper quartile.

In the four untreated and eight estradiol-treated baboons in which spiral artery volume flow was obtained by B-flow/STIC M-mode, median (IQR) volume flow was 85% lower in the SAR-suppressed compared with the untreated baboons (0.33 (0.17–1.01) mL *vs* 2.18 (1.00–2.75) mL per cardiac cycle; $P = 0.014$) (Figure 5).

DISCUSSION

The present study shows for the first time that B-flow/STIC M-mode ultrasonography provides a novel real-time non-invasive imaging method to detect a decrease in spiral artery luminal diameter, reflecting reduced distensibility of the vessel wall during the cardiac cycle, in the first trimester in a non-human primate model of impaired

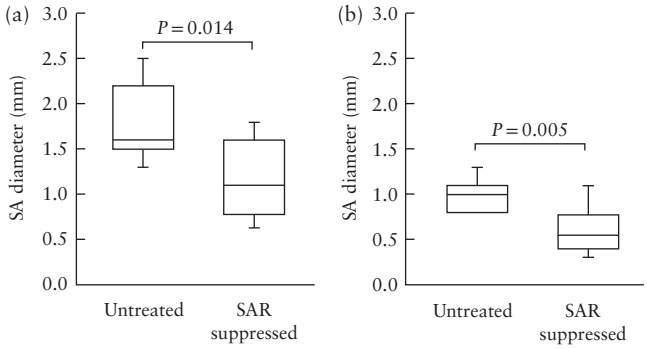

Figure 3 Box-and-whiskers plots showing spiral artery (SA) diameter in systole (a) and in diastole (b), as quantified by B-flow/STIC M-mode ultrasonography, on day 60 of gestation in seven untreated and 12 spiral artery remodeling (SAR)-suppressed baboons. Boxes are median and interquartile range and whiskers are range. In (b), the lowest value (0.8 mm) in the untreated group is also the first quartile (which is why there is no whisker).

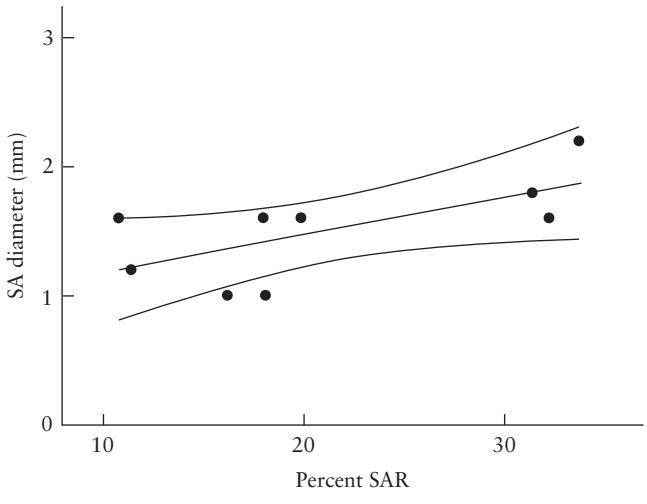

Figure 4 Correlation coefficient, with 95% CI, of spiral artery (SA) diameter in systole, as quantified by B-flow/STIC M-mode ultrasonography, and percent of spiral artery remodeling (SAR) (i.e. the number of trophoblast-invaded arteries divided by the total number of arteries counted), as quantified by immunohistochemical image analysis on day 60 of gestation, in three untreated and six SAR-suppressed baboons. $r = 0.67$; slope = 0.029 ($P < 0.05$).

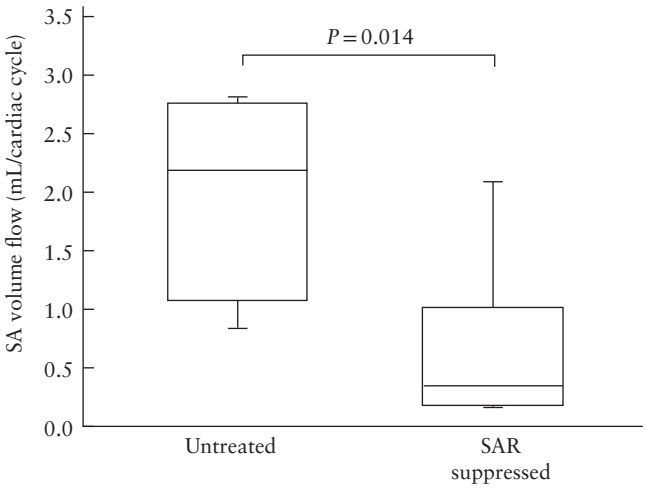

Figure 5 Box-and-whiskers plots showing spiral artery (SA) volume flow as quantified by B-flow/STIC M-mode ultrasonography on day 60 of gestation, in four untreated and eight spiral artery remodeling (SAR)-suppressed baboons. Boxes are median and interquartile range and whiskers are range.

SAR. Spiral artery luminal diameter, as quantified by B-flow/STIC M-mode imaging, was 31% lower in systole and 50% lower in diastole in SAR-suppressed baboons. The reduction in spiral artery luminal diameter was correlated with a decrease in the percent of spiral arteries remodeled by extravillous trophoblasts.

Although 3D power Doppler of the uteroplacental vascularization can identify some pregnancies at risk for pre-eclampsia[23–27], its prognostic value early in gestation is limited because power gain, pulse-repetition frequency and other 3D settings compromise imaging. Other Doppler approaches, for example coherent flow power Doppler and superb microvascular imaging, have been employed to quantify placental vascularization and flow[28,29], but the clinical utility of Doppler is compromised by 'blooming' artifacts, aliasing, signal drop-out and interference by fetal blood flow. In the present study, we employed B-flow/STIC M-mode ultrasonography, a non-Doppler technology that uses very short pulses with high spatiotemporal and contrast resolution to enable sharp rendering of vessel dimension. In the clinical setting, efficacy of a new imaging modality should be tested in a pilot case–control study and subsequently in a largescale population. We suggest that major strengths of the current study are the use of B-flow/STIC M-mode imaging and the use of a non-human primate pregnant model, in which real-time B-flow/STIC M-mode quantification of spiral artery luminal diameter was compared with *ex-vivo* quantification of the level of SAR by immunohistochemical image analysis in the first trimester of gestation, a stage at which such studies would be very difficult to undertake in human pregnancy.

We further suggest that the decrease in luminal diameter of the spiral arteries shown by B-flow/STIC M-mode imaging in the first trimester in SAR-suppressed baboons reflects the impairment of remodeling of the spiral arteries into enlarged vessels with distensible walls and not a change in some other aspect of blood vessel development, for example an estrogen-induced increase in vessel proliferation into more numerous blood vessels of smaller diameter. Indeed, the density of the uterine spiral arteries, i.e. the total number of blood vessels per area of decidua basalis, was unaltered by estradiol administration early in baboon pregnancy[30].

Because the rate of blood flow through a vessel is proportional to the fourth power of vessel diameter[31], the 31–50% decrease in spiral artery diameter, as observed by B-flow/STIC M-mode in SAR-suppressed baboons, would be expected to result in a marked reduction in blood flow and placental perfusion. Indeed, the present study shows that spiral artery volume flow was 85% lower in SAR-suppressed compared with normal baboons in the first trimester. In contrast, we showed previously that uterine artery volume flow, as quantified by Doppler ultrasound, was similar on day 60 of gestation in untreated (2.91 ± 0.38 mL/min/kg of body weight) and estradiol-treated/SAR-suppressed (2.90 ± 0.65 mL/min/kg of body weight) baboons, although Doppler was able to show an increase in downstream flow resistance near term in the SAR-suppressed animals[11]. Although an elevation in blood pressure can increase blood flow through the systemic vasculature, maternal arterial blood pressure was unaltered early in pregnancy but became elevated by over 25% near term in SAR-impaired baboons[11,13].

Along with the suppression of SAR, maternal vascular endothelial dysfunction was induced late in gestation in our baboon experimental model[13]. The latter pathophysiological manifestation is a hallmark of human pre-eclampsia[32–36]. Placental and fetal body weights of SAR-impaired baboons were not altered in the first (Table 1) and third[11] trimesters of pregnancy, despite the reduction in spiral artery volume flow and onset of maternal vascular dysfunction[13]. However, near term and after birth, offspring derived from SAR-impaired baboons appear to exhibit systemic vascular dysfunction (unpublished preliminary data), which has also been shown in offspring from human pregnancies with pre-eclampsia[37]. Therefore, we propose that the current results obtained in a non-human primate translate to human pregnancy and indicate that B-flow/STIC M-mode ultrasonography provides a novel, safe and real-time imaging technology to quantify aspects of spiral artery dynamics that reflect the process of SAR. Future studies will ascertain whether B-flow/STIC M-mode ultrasonography will uncover a deficiency in spiral artery luminal diameter reflective of SAR impairment early in gestation in women who go on to exhibit the pathophysiological conditions associated with abnormal pregnancy, such as pre-eclampsia.

We have reported recently that non-invasive targeted delivery of the vascular endothelial growth factor (VEGF) gene selectively to the maternal aspect of the placenta (but not the fetus) by contrast-enhanced ultrasound-mediated cavitation of acoustically active microbubble prevented

the impairment of SAR as quantified by immunohistochemical analysis in estradiol-treated baboons[12]. The latter study showed that VEGF has a pivotal role in promoting spiral artery transformation during the first trimester of primate pregnancy. Future studies can be designed to ascertain whether detection of impairment of SAR by non-invasive B-flow/STIC M-mode ultrasound combined with targeted delivery of the VEGF gene early in pregnancy in estradiol-treated baboons provides an effective therapeutic intervention to prevent abnormal pregnancy. Positive results of such a study in the pregnant baboon would provide a basis for translational investigation of this treatment paradigm in adverse conditions of human pregnancy underpinned by improper SAR.

In conclusion, the present study shows that B-flow/STIC M-mode ultrasonography provides a novel real-time imaging method to detect a decrease in uterine spiral artery luminal diameter during the cardiac cycle in early pregnancy in a non-human primate model of impaired SAR.

ACKNOWLEDGMENTS

We thank Irene Baranyk, B.A., for the computer-assisted preparation of this manuscript and Sandra Huband, B.A, for the computer-assisted preparation of the graphs. This study was supported by NIH R01 HD 93070 and R01 HD 93946 research grants.

REFERENCES

1. Brosens I. A study of the spiral arteries of the decidua basalis in normotensive and hypertensive pregnancies. *J Obstet Gynaecol Br Commonw* 1964; **71**: 222–230.
2. Lyall F, Robson SC, Bulmer JN. Spiral artery remodeling and trophoblast invasion in preeclampsia and fetal growth restriction: relationship to clinical outcome. *Hypertension* 2013; **62**: 1046–1054.
3. Burton GJ, Fowden AL, Thornburg KL. Placental origins of chronic disease. *Physiol Rev* 2016; **96**: 1509–1565.
4. Llurba E, Turan O, Kasdaglis T, Harman CR, Baschat AA. Emergence of late-onset placental dysfunction: relationship to the change in uterine artery blood flow resistance between the first and third trimesters. *Am J Perinatol* 2013; **30**: 505–512.
5. Song WL, Zhao YH, Shi SJ, Liu XY, Zheng GY, Morosky C, Jiao Y, Wang XJ. First trimester Doppler velocimetry of the uterine artery ipsilateral to the placenta improves ability to predict early-onset preeclampsia. *Medicine (Baltimore)* 2019; **98**: e15193.
6. Taylor TJ, Quinton AE, deVries BS, Hyett JA. Uterine artery pulsatility index assessment at < 11 weeks' gestation: a prospective study. *Fetal Diagn Ther* 2020; **47**: 129–137.
7. Benirschke K, Kaufmann P. *Pathology of the Human Placenta*. Springer-Verlag: New York, NY, 2000; 220–223.
8. Bonagura TW, Pepe GJ, Enders AC, Albrecht ED. Suppression of extravillous trophoblast vascular endothelial growth factor expression and uterine spiral artery invasion by estrogen during early baboon pregnancy. *Endocrinology* 2008; **149**: 5078–5087.
9. Bonagura TW, Babischkin JS, Aberdeen GW, Pepe GJ Albrecht ED. Prematurely elevating estradiol in early baboon pregnancy suppresses uterine artery remodeling and expression of extravillous placental vascular endothelial growth factor and α1β1 and α5β1 integrins. *Endocrinology* 2012; **153**: 2897–2906.
10. Albrecht ED, Pepe GJ. Endocrinology of pregnancy. In *Non-Human Primates in Perinatal Research*, Brans YW, Kuehl TJ (eds). John Wiley & Sons: New York, NY, 1988; 13–78.
11. Aberdeen GW, Bonagura TW, Harman CR, Pepe GJ, Albrecht ED. Suppression of trophoblast uterine spiral artery remodeling by estrogen during baboon pregnancy: impact on uterine and fetal blood flow dynamics. *Am J Physiol Heart Circ Physiol* 2012; **302**: H1936–H1944.
12. Babischkin JS, Aberdeen GW, Lindner JR, Bonagura TW, Pepe GJ, Albrecht ED. Vascular endothelial growth factor delivery to placental basal plate promotes uterine artery remodeling in the primate. *Endocrinology* 2019; **160**: 1492–1505.
13. Albrecht ED, Babischkin JS, Aberdeen GW, Burch MG, Pepe GJ. Maternal systemic vascular dysfunction in a primate model of defective uterine spiral artery remodeling. *A J Physiol Heart Circ Physiol* 2021; **320**: H1712–H1723.
14. Turan S, Turan O, Baschet AA. Three- and four-dimensional fetal echocardiography. *Fetal Diagn Ther* 2009; **25**: 361–372.
15. Hongmei W, Ying Z, Ailu C, Wei S. Novel application of four-dimensional sonography with B-flow imaging and spatiotemporal image correlation in the assessment of fetal congenital heart defects. *Echocardiography* 2012; **29**: 614–619.
16. Dighe MK, Moshiri M, Jolley J, Thiel J, Hippe D. B-flow imaging of the placenta: a feasibility study. *Ultrasound* 2018; **26**: 160–167.
17. Percie du Sert N, Hurst V, Ahluwalia A, Alam S, Avey MT, Baker M, Browne WJ, Clark A, Cuthill IC, Dirnagl U, Emerson M, Garner P, Holgate ST, Howells DW, Karp NA, Lazic SE, Lidster K, MacCallum CJ, Macleod M, Pearl EJ, Petersen OH, Rawle F, Reynolds P, Rooney K, Sena ES, Silberberg SD, Steckler T, Würbel H. The ARRIVE guidelines 2.0: Updated guidelines for reporting animal research. *PLoS Biol* 2020; **18**: e3000410.
18. National Research Council (US) Committee for the Update of the Guide for the Care and Use of Laboratory Animals. *Guide for the Care and Use of Laboratory Animals* (8th edn). National Academies Press (US): Washington DC; 2011.
19. Urbaniak GC, Plous S. Research randomizer version 4.0 computer software, 2013. http://www.randomizer.org.
20. Houston ML, Hendrickx AG. Observations on the vasculature of the baboon placenta (*Papio* sp.) with special reference to the transverse communicating artery. *Folia Primatol* 1968; **9**: 68–77.
21. Ramsey EM, Donner MW. Structure of the chorionic villi. In *Placental Vasculature and Circulation*, Ramsey EM, Donner MW (eds). W.B. Saunders Company: Philadelphia, PA, 1980; 31.
22. Balasuriya H, Bell P, Waugh R, Thompson J, Gillin A, Hennessy A, Makris A. Primate maternal placental angiography. *Placenta* 2010; **31**: 11–22.
23. Dar P, Gebb J, Reimers L, Bernstein PS, Chazotte C, Merkatz IR. First-trimester 3-dimensional power Doppler of the uteroplacental circulation space: a potential screening method for preeclampsia. *Am J Obstet Gynecol* 2010; **203**: 238.e1–7.
24. Rosner M, Dar P, Reimers LL. First-trimester 3D power Doppler of the uteroplacental circulation space and fetal growth restriction. *Am J Obstet Gynecol* 2014; **211**: 521.e1–8.
25. Hashish N, Hassan A, El-Semary A, Gohar R, Youssef MA. Could 3D placental volume and perfusion indices measured at 11–14 weeks predict occurrence of preeclampsia in high-risk pregnant women? *J Matern Fetal Neonatal Med* 2015; **28**: 1094–1098.
26. Neto RM, Ramos JG. 3D power Doppler ultrasound in early diagnosis of preeclampsia. *Pregnancy Hypertens* 2016; **6**: 10–16.
27. Eastwood KA, Patterson C, Hunter AJ, McCance DR, Young IS, Holmes VA. Evaluation of the predictive value of placental vascularization indices derived from 3-dimensional power Doppler whole placental volume scanning for prediction of pre-eclampsia: a systemic review and meta-analysis. *Placenta* 2017; **51**: 89–97.
28. Li YL, Dahl JJ. Coherent flow power Doppler (CFPD): flow detection using spatial coherence beamforming. *IEEE Trans Ultrason Ferroelectr Freq Control* 2015; **62**: 1022–1035.
29. Artul S, Nseir W, Armaly Z, Soudack M. Superb microvascular imaging: added value and novel applications. *J Clin Imaging Sci* 2017; **7**: 45.
30. Albrecht ED, Bonagura TW, Burleigh DW, Enders AC, Aberdeen GW, Pepe GJ. Suppression of extravillous trophoblast invasion of uterine spiral arteries by estrogen during early baboon pregnancy. *Placenta* 2006; **27**: 483–490.
31. Guyton AC, Hall JE. *Guyton and Hall Textbook of Medical Physiology* (12th edn). Saunders Elsevier: Philadelphia, PA, 2011.
32. Roberts JM, Taylor RN, Musci TJ, Rodgers GM, Hubel CA, Mclaughlin MK. Preeclampsia: an endothelial cell disorder. *Am J Obstet Gynecol* 1989; **161**: 1200–1204.
33. Gilbert JS, Ryan MJ, LaMarca BB, Sedeek M, Murphy SR, Granger JP. Pathophysiology of hypertension during preeclampsia: linking placental ischemia with endothelial dysfunction. *Am J Physiol Heart Circ Physiol* 2008; **294**: H541–550.
34. Myatt L, Webster RP. Vascular biology of preeclampsia. *J Thromb Haemost* 2009; **7**: 375–384.
35. Ilekis JV, Tsilou E, Fisher S, Abrahams VM, Soares MJ, Cross JC, Zamudio S, Illsley NP, Myatt L, Colvis C, Costantine MM, Haas DM, Sadovsky Y, Weiner C, Rytting E, Bidwell G. Placental origins of adverse pregnancy outcomes: potential molecular targets: an executive workshop summary of the Eunice Kennedy Shriver National Institute of Child Health and Human Development. *Am J Obstet Gynecol* 2016; **215** (1 Suppl): S1–S46.
36. Rana S, Lemoine E, Granger JP, Karumanchi SA. Preeclampsia: pathophysiology, challenges, and perspectives. *Circ Res* 2019; **124**: 1094–1112.
37. Fox R, Kitt J, Leeson P, Aye CYL, Lewandowski AJ. Preeclampsia: risk factors, diagnosis, management, and the cardiovascular impact on the offspring. *J Clin Med* 2019; **8**: 1625.